Hindawi Publishing Corporation
Journal of Nanomaterials
Volume 2016, Article ID 4024527, 8 pages
http://dx.doi.org/10.1155/2016/4024527

Research Article

Isolation and Characterization of Cellulose Nanofibers from *Gigantochloa scortechinii* as a Reinforcement Material

Chaturbhuj K. Saurabh,[1] Asniza Mustapha,[1] M. Mohd. Masri,[1] A. F. Owolabi,[2] M. I. Syakir,[1] Rudi Dungani,[3] M. T. Paridah,[4] M. Jawaid,[4] and H. P. S. Abdul Khalil[1]

[1]*School of Industrial Technology, Universiti Sains Malaysia, 11800 Penang, Malaysia*
[2]*Federal Institute of Industrial Research Oshodi, Lagos 25016, Nigeria*
[3]*School of Life Sciences and Technology, Gandung Labtex XI, Institut Teknologi Bandung, Bandung 40132, Indonesia*
[4]*Institute of Tropical Forestry & Forest Products, Universiti Putra Malaysia, 43400 Serdang, Malaysia*

Correspondence should be addressed to H. P. S. Abdul Khalil; akhalilhps@gmail.com

Received 28 April 2016; Revised 3 June 2016; Accepted 16 June 2016

Academic Editor: Zeeshan Khatri

Copyright © 2016 Chaturbhuj K. Saurabh et al. This is an open access article distributed under the Creative Commons Attribution License, which permits unrestricted use, distribution, and reproduction in any medium, provided the original work is properly cited.

Cellulose nanofibers (CNF) were isolated from *Gigantochloa scortechinii* bamboo fibers using sulphuric acid hydrolysis. This method was compared with pulping and bleaching process for bamboo fiber. Scanning electron microscopy, transmission electron microscopy, Fourier transform infrared spectroscopy, X-ray diffraction, and thermogravimetric analysis were used to determine the properties of CNF. Structural analysis by FT-IR showed that lignin and hemicelluloses were effectively removed from pulp, bleached fibers, and CNF. It was found that CNF exhibited uniform and smooth morphological structures, with fiber diameter ranges from 5 to 10 nm. The percentage of crystallinity was significantly increased from raw fibers to cellulose nanofibers, microfibrillated, along with significant improvement in thermal stability. Further, obtained CNF were used as reinforcement material in epoxy based nanocomposites where tensile strength, flexural strength, and modulus of nanocomposites improved with the addition of CNF loading concentration ranges from 0 to 0.7%.

1. Introduction

Over the years, numerous studies have been performed to find the ideal cellulosic reinforcing material from natural plant fibers. Bamboo is possibly an ideal source for cellulose based nanofibers. It is a fast growing plant and widely considered as an excellent source of cellulose fibers that possess relatively small microfibrillar angles and high cellulose content [1]. Malaysia is endowed with more than 50 bamboo species. Among these, almost 14 species are commercially exploited [2]. *Gigantochloa* genus is one of the most utilized bamboos in Malaysia due to its uniformity in size, thick culms wall, and ease of cultivation, which makes this bamboo genus a good choice for industrial usage [3].

Studies on cellulosic plant fibers for various applications are widely done since they are sustainable, green, and environmental friendly. Easy processing, low cost, low energy consumption, light weight, excellent specific strength, low environmental hazard, and renewability and recyclability of the reinforced green composite have generated great interest among researchers over conventional synthetic reinforced fibers [4, 5]. The utilization of bamboo fibers in composites has attracted interest because of its biodegradability and clean emissions [6, 7]. The incorporation of bamboo fiber improves certain properties of the polymer composite matrix (i.e., fracture toughness and impact behavior); however, flexural strength of composites was not significantly affected [8–10]. It is believed that the poor compatibility between the cellulose and polymer matrix causes the low flexural strength in cellulose reinforced composite materials. The poor matrix accessibility increases the interfacial tension between cellulose fibers and polymeric matrices, thus increasing the porosity of composites [11, 12]. Thus there is need to develop a novel methodology for the production of cellulose fibers which have better compatibility with the polymeric matrices.

Cellulose is a biopolymer. It is the main component of all plant fibers and composed of repeating units of β-D-glucose [13]. Nanoscale cellulose fibers can be isolated from various cellulosic sources by a number of isolation methods, including various mechanical treatments which can be used in combination or independently. Researchers have combined mechanical processes such as refining [14] and cryocrushing [15] with pretreatment of cellulosic fiber by means of physical, chemical, or enzymatic hydrolysis [7, 10, 16, 17] to improve the mechanical and barrier properties of extracted bamboo fiber-reinforced composites.

Combination of sulphuric acid hydrolysis and homogenization methods to isolate CNF is reported to be convenient and had minimum effect on fiber properties [18]. However, isolation and characterization of CNF from *Gigantochloa scortechinii* using a combination of pulping, bleaching, and hydrolysis has not been previously reported. Therefore, the present study was conducted to isolate CNF from *Gigantochloa scortechinii* fibers using the above combined procedures together known as a chemomechanical process. Several analytical techniques, including scanning electron microscopy (SEM), transmission electron microscopy (TEM), Fourier transform infrared spectroscopy (FT-IR), X-ray diffraction (XRD), and thermogravimetric analysis (TGA), were used to characterize the morphology, structure, crystallinity, and thermal properties of isolated nanofibers. After successful isolation of CNF it was incorporated in epoxy resin at different concentrations to study the effect of CNF as a reinforcing agent on mechanical properties of nanocomposites.

2. Materials and Methods

2.1. Materials. *Gigantochloa scortechinii* bamboo culms were collected from Forest Research Institute of Malaysia (FRIM), Kepong, Selangor, Malaysia. The bamboo culms were cut into small pieces (size of 1.5 cm^2) and dried until the overall moisture content of samples reaches 5 ± 0.2%. The moisture content was measured using MB45 Moisture Analyzer. In present study sodium hydroxide (NaOH), anthraquinone (AQ), hydrogen peroxide (H_2O_2), magnesium sulphate ($MgSO_4$), sulphuric acid (H_2SO_4) and other chemicals of analytical grade were received from Bumificient Sdn Bhd, Kuala Lumpur, Malaysia, and used without any processing.

2.2. Soda-AQ Pulping. Pulping of dried bamboo chips was performed in an "Ibsutek Zat 92" (RB Supply Enterprise, Penang, Malaysia) 20 L stainless steel rotary digester with 25% (w/w) NaOH and 0.1% (w/w) AQ as cooking liquor. The cooking temperature and time were 170°C and 3 h, respectively, and the ratio of cooking liquor to bamboo fiber was 7 : 1 (v/w). After pulping, bamboo pulps were washed thoroughly with distilled water to eliminate residues of cooking liquor. Samples were oven-dried at 60°C for 24 hours.

2.3. Alkaline-Peroxide Bleaching. Bamboo pulps were subjected to alkaline-peroxide bleaching process. 12 g of pulp was treated with 52.42 mL of aqueous solution containing 3% (v/v) H_2O_2, 3% (w/w) NaOH, and 0.5% (w/w) $MgSO_4$ at 80°C for 2 h. Upon completion of bleaching slurry was rinsed with water and oven-dried at 60°C for 24 h prior to storage.

2.4. Isolation of Cellulose Nanofibers. 10 g of bleached pulps was hydrolyzed in sulphuric acid (H_2SO_4) aqueous solution (30%, v/v) under strong agitation at 90°C for 2 h. The ratio of acid over bleached pulp was 20 : 1. Hydrolysis was terminated by adding excess of cold distilled water into mixture and diluted suspension was centrifuged at 11,000 rpm for 10 min. The collected precipitate was resuspended in distilled water under strong agitation. This process was repeated until pH reached to 7. Finally obtained precipitate was soaked in distilled water and subjected to 20 min of homogenization followed by sonication for 30 min to isolate nanofibers. Finally, slurry was freeze-dried prior to characterization of nanofibers.

2.5. Preparation of CNF Reinforced Epoxy Nanocomposites. Extracted CNF from *G. scortechinii* was used as filler or reinforcement in epoxy based nanocomposites. Epoxy resin (100 phr) and polyamine hardener (60 phr) were mixed as matrix. Nanocomposites were fabricated using different CNF loading percentages of 0.3%, 0.5%, and 0.7% (w/w). CNF was added to epoxy resin mixture at different concentrations and stirred by using mechanical stirrer for 30 min at room temperature. Bubbles from the mixture were removed by using vacuum chamber for 30 min. Polyamine hardener 8161 as a curing agent was then added to the mixture and mechanically stirred for 10 min. The mixture was again degassed in vacuum chamber for 15 min. Subsequently, the obtained solution was casted into a mould (160 mm × 160 mm × 3 mm) which was covered with silicon oil as a releasing agent. Finally, the composite was cured at 85°C for 2 hr and continued for postcure at 125°C for 3 hr.

2.6. Characterization. Various properties of extracted CNF were evaluated by SEM, TEM, FT-IR, XRD, and TGA. Morphology was analyzed via SEM (EVO MA10; Carl Zeiss SMT, Germany). The acceleration voltage was set at 15 kV, and fibers were coated with a very thin layer of gold prior to analysis.

TEM of the resultant suspension of CNF was performed on a Libra 120, Carl Zeiss (Germany) electron microscope at an acceleration voltage of 120 kV. CNF was diluted in distilled water (0.01% of w/v). Carbon-coated grid was used to deposit a drop of diluted CNF suspension. Diameter of CNF was measured by image analysis system (Image Pro Plus ver. 7.01; Media Cybernetics, Inc., USA). Dimensions were calculated from the measurement of dozens of nanofibers and mean value was reported as diameter of that sample.

Change in functional groups of samples was determined by using Fourier transform infrared (FT-IR) spectroscopy (IS10 Nicolet, Thermo Scientific, USA) in range of 400–4000 cm^{-1} with a resolution of 4 cm^{-1}. Samples were grounded into powder and blended with high-purity dried potassium bromide (KBr) before pressing into ultrathin transparent pellets.

Crystallinity percentage of raw bamboo fiber, pulp, bleached pulp, and CNF was determined by using an X-ray diffractometer (D8 Advanced Bruker, Germany) at 2θ range from 5° to 50°. Crystallinity percentage was calculated based on the following equation:

$$C_{IR}\,(\%) = \frac{I_{200} - I_{AM}}{I_{200}} \times 100, \quad (1)$$

where I_{200} signifies amorphous and crystalline fractions and I_{AM} signifies amorphous region.

Degradation temperature and thermal stability of cellulose fibers were analyzed by using thermogravimetric analyzer (TGA/SDTA 851; Mettler Toledo, Switzerland). All samples were heated from 30°C to 800°C under nitrogen atmosphere at a heating rate of 20°C/min.

Mechanical properties of neat composite and CNF reinforced epoxy nanocomposites were analyzed by using Instron 5582 universal testing machine (USA). Tensile modulus and tensile strength was determined by ASTM-D3039. In short all samples were cut into dimension of 120 mm × 15 mm × 3 mm. Testing speed and gauge length were set at 5 mm/min and 60 mm, respectively. Flexural test was conducted by three-point bending test based on ASTM-D790. All samples were cut into dimension of 160 mm × 20 mm × 3 mm and the crosshead speed was set at 2 mm/min.

Fractured surface of nanocomposites were observed using SEM (EVO MA10; Carl Zeiss SMT, Germany) with accelerating voltage at 15 kV. Samples with thickness of 2 mm from tensile test were sputtered with gold prior to observation in order to avoid surface changing during the test.

3. Results

3.1. Morphological Analysis. Surface morphology and size of fibers might change during chemical and mechanical pretreatment. Figure 1 shows the SEM images of raw bamboo fiber, pulp, bleached pulp, and acid hydrolyzed fiber. It is evident from SEM images that the morphology of treated bamboo fiber changed during processing. Raw bamboo fiber is composed of bundles with continuous individual cells that are bound together by cemented components of lignin, hemicelluloses, and waxy materials [3]. Thus, typically rough and irregular surface of raw bamboo fiber (Figure 1(a)) was due to the presence of noncellulosic materials [16, 17]. The surface of fibers appears to be uniform and smooth in SEM image of pulp, bleached pulp, and hydrolyzed fiber (Figures 1(b), 1(c), and 1(d)) due to removal of noncellulosic materials.

Pulping is known to liberate individual fibers from fiber bundles; however, single fibers of pulp still tangled with each other. Subsequent bleaching treatment resulted in smoother and clear surface of fibers with significant decrease in diameter. TEM images of CNF (Figures 1(e) and 1(f)) showed individual nanofibers with little agglomeration. The diameter of raw fiber, pulp, bleached pulp, and cellulose nanofiber ranged between 79.86 and 183.1 μm, 16.87 and 23.27 μm, 8.94 and 18.57 μm, and 5.29 and 10.94 nm, respectively. Other study on CNF from different species of bamboo exhibited lateral size of 10 to 30 nm [19]. Thus nanofibers generated in the present study had lower diameter than CNF of already reported literature. It is apparent that soda pulping, alkaline-peroxide bleaching, and acid hydrolysis process effectively removed noncellulosic components and thus reducing fiber dimension. Chemomechanical treatments separated raw fibers into individual micron-to-nanosized fibers.

3.2. Fourier Transform Infrared Spectrometry Analysis. FT-IR spectroscopy was used to evaluate the changes in functional groups of fibers at different stages of treatment. FT-IR spectra of raw fiber, pulp, bleached pulp, and CNF are shown in Figure 2. Strong and broad band at 3413 cm^{-1} was attributed to stretching vibration of hydroxyl groups (-OH). Band at 2904 cm^{-1} was ascribed to C-H stretching. Bands at 1732 cm^{-1}, 1621 cm^{-1}, 1509 cm^{-1}, 1435 cm^{-1}, 1370 cm^{-1}, and 1160 cm^{-1} corresponded to C=O stretching in hemicellulose, absorbed water, aromatic asymmetric stretching of lignin, bending vibration of CH_2 groups, C-H groups of aromatic ring, and C-O-C linkages in lignin, respectively [16, 20]. Furthermore, absorption peak that can be seen around 1035 cm^{-1} was assigned to stretching of O-H and C-H groups, whereas vibrational peak at 828 cm^{-1} was due to characteristic of β-glycosidic bond [21].

Reduction in intensity of peaks or disappearance of any peak in FT-IR analysis would give good information about changing in functional groups of samples at different stages of treatment. Disappearance of peaks from 1732 cm^{-1}, 1509 cm^{-1}, and 1251 cm^{-1} in pulp, bleached pulp, and CNF confirmed the removal of lignin and hemicelluloses from raw fibers during soda pulping, alkaline-peroxide bleaching, and acid hydrolysis. These treatments caused the reduction of strong and broad bands from control sample, especially stretching vibration band between 3000 and 3500 cm^{-1}, which demonstrated the removal of phenolic and alcoholic waxy materials from fibers.

3.3. X-Ray Diffraction Analysis. Crystalline behavior of cellulose fibers was measured by XRD analysis. Figure 3 illustrates the X-ray diffractogram of raw fiber, pulp, bleached pulp, and CNF from *G. scortechinii*. Cellulose contains partially crystalline and amorphous structure resulting from the placement of glycosidic chain, which is held closely by mutual H-bonding in the crystalline region and absence of such organized H-bonding in amorphous region [22]. Results showed that peaks at around 2θ = 15° and 22.5°, which are believed to represent the typical native cellulose crystalline structure [23], indicated that the crystal integrity of fibers had been maintained during treatment.

Crystallinity of cellulosic bamboo fiber was determined at every stage of treatment. It was observed that the crystallinity is significantly affected by each process. The crystallinity values of raw fiber, pulp, bleached pulp, and CNF was 47.91%, 54.34%, 60.89%, and 65.32%, respectively. Value of crystallinity increased after each chemical treatment, which might have resulted from the dissolution and removal of noncellulosic components including lignin and hemicelluloses that present in amorphous regions of raw fibers. Thus,

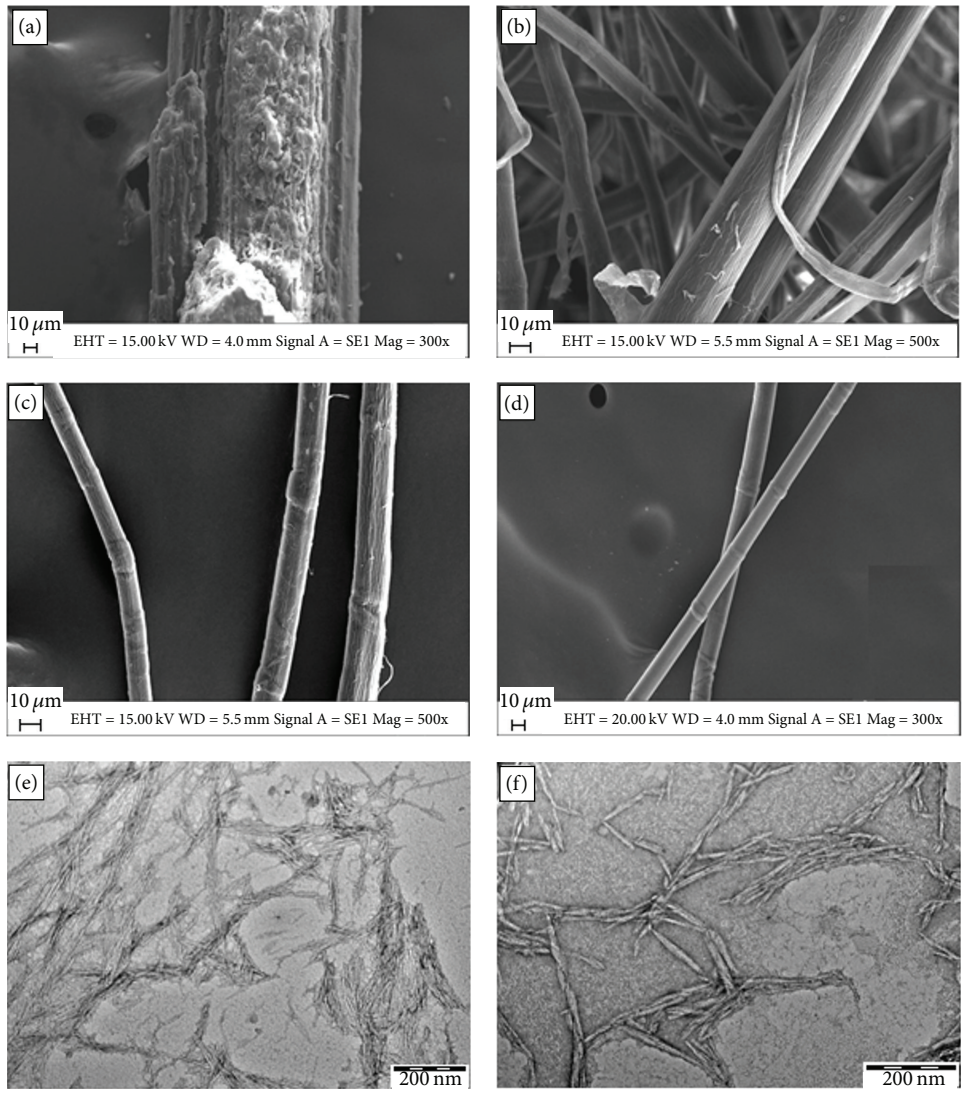

Figure 1: (a) SEM micrographs of raw fiber; (b) SEM micrographs of pulp; (c) SEM micrographs of bleached pulp; (d) SEM micrographs of acid hydrolysis treated fiber; and (e, f) TEM micrographs of CNF.

with each step, degree of crystallinity in fibers increases with subsequent exclusion of amorphous parts from samples.

3.4. Thermal Properties Analysis. Thermal stability of reinforcing material is important to determine their applicability for biocomposite processing at high temperature [24]. TGA thermograms of *G. scortechinii's* fiber from each treatment process are shown in Figure 4. The curves illustrate an initial weight of 7% from all fibers occurring between 30 and 100°C, due to evaporation of absorbed moisture. Thermal characteristics, including initial decomposition temperature (T_{Onset}), maximum degradation temperature (T_{max}), and percentage of residue at 800°C of all the samples, are summarized in Table 1. T_{Onset} values of raw fiber, pulp, bleached pulp, and CNF were found to be 306, 332, 344, and 345°C, respectively. The second stage of mass loss, which was in the range of 200–450°C, corresponded to decomposition of cellulose, hemicelluloses, and lignin. The maximum degradation temperature (T_{max}) values were 351, 365, 370, and 376°C for the raw fiber, pulp, bleached pulp, and CNF, respectively. Pulping, bleaching, and hydrolysis reduced the overall char residue from raw fibers. It was observed that the amount of residues present at 800°C was reduced from 33% of raw fiber to 8% in nanofibers. Residue percentage decreases throughout the treatment process. A higher amount of residue in the raw fibers directly correlates to the presence of lignin, hemicelluloses, and other noncellulosic materials. During treatment subsequent loss of noncellulosic material occurred which resulted in lower residue percentage.

Thermal stability increased after chemomechanical treatment, which was due to the removal of hemicelluloses and lignin. Increase in fiber crystallinity was confirmed by higher value of T_{max}. During acid hydrolysis amorphous region in cellulose might get disintegrated and subsequent increase in degree of crystallinity was observed. The higher crystallinity leads to greater heat resistance, thus boosting the thermal

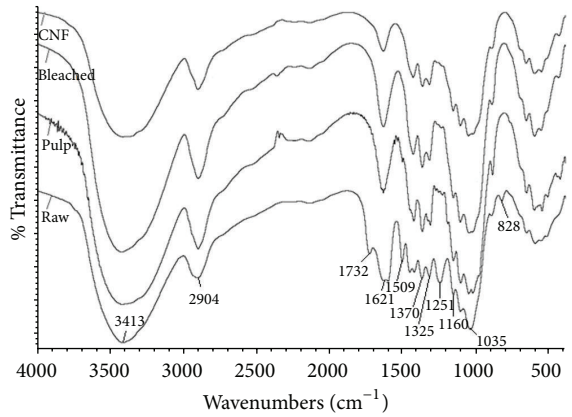

Figure 2: FT-IR spectra of raw fiber, pulp, bleached pulp, and CNF from *G. scortechinii*.

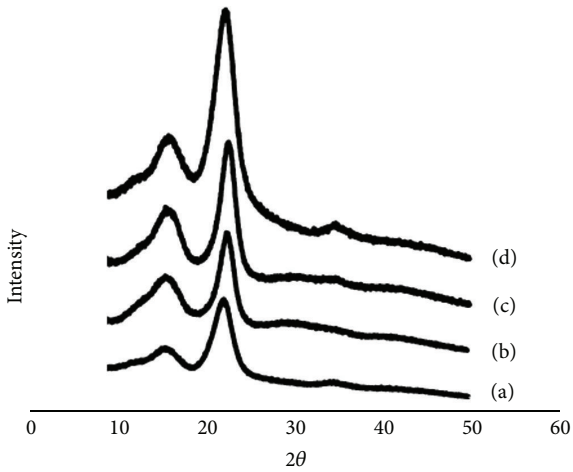

Figure 3: XRD diffractograms of (a) raw fiber; (b) pulp; (c) bleached pulp; and (d) CNF.

Table 1: Thermal properties of treated cellulose fibers at each step.

Sample	T_{Onset} (°C)	T_{max} (°C)	Residue (%)
Raw fiber	258.77	351.51	33.90
Pulp	243.81	365.10	23.38
Bleached pulp	344.60	370.42	11.01
Cellulose nanofibers	345.32	376.39	8.36

stability [22]. Higher crystallinity induces more ordered cellulose regions. More densely packed cellulose chains in a highly organized form can lead to higher hydrogen bond intensity between neighboring cellulose chains; thus, this might hinder heat transfer by diffusion through cellulose chains. High thermal stability of CNF as observed in present study is important for reinforcement agent in functional composites applications.

3.5. Mechanical Properties of Nanocomposites. Tensile and flexural properties of neat epoxy composites and CNF reinforced epoxy based nanocomposites are tabulated in Table 2.

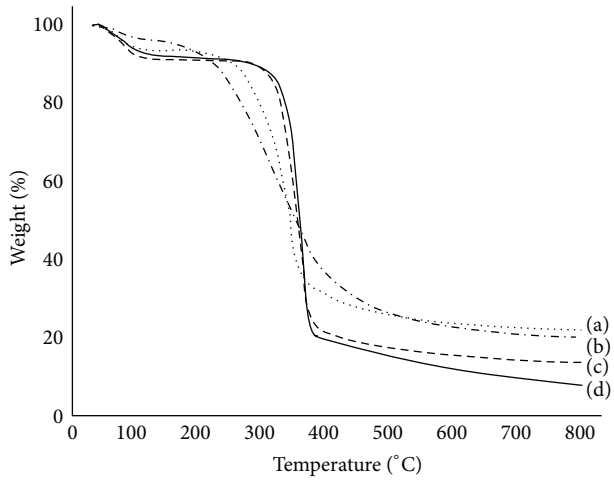

Figure 4: TGA thermograms of (a) raw fiber; (b) pulp; (c) bleached pulp; and (d) CNF.

Tensile strength and modulus of nanocomposites increased from 24.1 to 31.3 MPa and 0.78 to 1.3 GPa, respectively, with increase in CNF concentration from 0 to 0.7%. Observed improvement in tensile strength and modulus was a result of high surface area of reinforcing agent which promotes good interfacial bonding between CNF nanofiller and epoxy matrix. Thus it prevents rapid crack propagation and provides better stress transmit and subsequently improved elastic deformation. Similarly, flexural strength and modulus of nanocomposites were also improved due to incorporation of CNF in epoxy resin at all concentrations studied in present work. Earlier, CNF was introduced and demonstrated to improve the mechanical performance of various kinds of polymer matrix based composites as reported by various other researchers [25–27]. Nanocomposites significantly exhibit good mechanical properties than the neat polymer even at low CNF reinforcement concentration. However, CNF loading caused reduction in elongation at break from 6.84% of neat epoxy to 3.34% of 0.7% CNF incorporated composite. Reduction in elongation at break might be due to the probability of fiber aggregation which resulted in area of stress concentrations that require less energy to propagate cracks and fracture. Hence, during tensile deformation, stress cannot transfer efficiently near these flaws and thus resulted in failure. Furthermore, high rigidity of CNF also contributed to the reduction in elongation at break.

3.6. Fracture Surface Morphology. SEM micrographs in Figure 5 represent the tensile fractured surface of CNF reinforced epoxy based nanocomposites. The interface bonding, crack propagation, and dispersion of bamboo CNF in the matrix were observed. The surface of 0% CNF loading/neat epoxy was smooth, which indicated the brittle nature of neat epoxy composite. Brittleness of pure epoxy resulted in its low resistance against crack propagation, thus having low mechanical strength. Images of CNF loaded nanocomposites exhibited rough fractured surfaces with the presence of white dots that represent CNF in nanocomposites. Moreover,

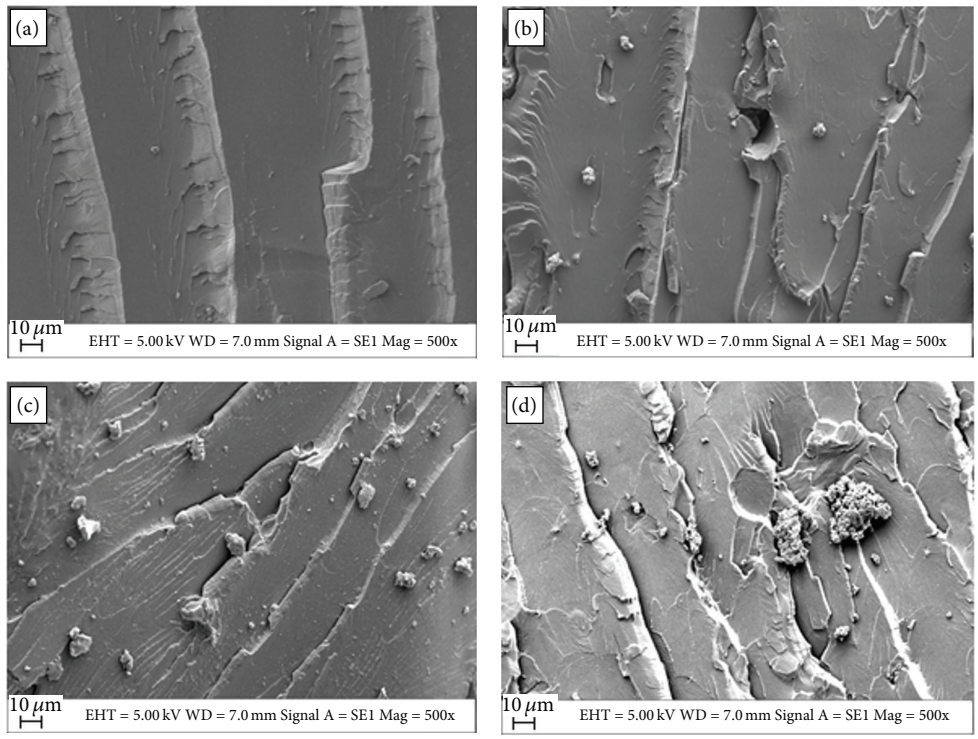

Figure 5: SEM micrographs of tensile fracture surfaces of (a) neat epoxy; (b) 0.3% CNF; (c) 0.5% CNF; and (d) 0.7% CNF reinforced epoxy based nanocomposites.

Table 2: Mechanical properties of CNF reinforced epoxy based nanocomposites.

CNF loading (% w/w)	Tensile			Flexural	
	Strength (MPa)	Modulus (GPa)	Elongation (%)	Strength (MPa)	Modulus (GPa)
0	24.10	0.78	6.84	24.50	1.12
0.3	25.60	0.93	5.81	26.93	1.17
0.5	28.20	1.17	4.12	29.40	1.21
0.7	31.30	1.30	3.34	32.00	1.36

brittleness of fractured surface of nanocomposites can be proved by the presence of sharp edges and deep line markings between the fractured surfaces. This justifies the observed reduction in elongation at break with CNF content in epoxy resin. Thus it was revealed by the analysis of SEM images that 0.3% CNF loaded fracture surface showed less brittleness as compared to 0.5% and 0.7% CNF incorporated composites. In 0.5% and 0.7% CNF loaded epoxy composites the crack propagation was rapid, thus resulting in roughness and deep line marking on both surfaces. However, there were no obvious agglomerates observed on the fracture surfaces of 0.5% CNF as compared to 0.7% CNF incorporated epoxy composites, which might be attributed to the good dispersion and distribution of CNF without aggregation. Better dispersion resulted in improved tensile strength and modulus as observed in the present study.

Furthermore, deep line marking was observed and the surface became rough with the addition of 0.7% CNF in epoxy resin. As the concentration of CNF in matrix increased little agglomeration was observed. The presence of agglomeration was probably due to poor dispersion and distribution of CNF in the nanocomposite. The agglomeration might lead to improper interfacial bonding between reinforcement material and the matrix [28]. As Masoodi et al. [29] reported, absorbed moisture in CNF also resulted in improper bonding between CNF and epoxy during curing process. On the other hand, Omrani et al. [25] found that low amount of CNF loading in epoxy based nanocomposites resulted in smooth surface as observed in present study. Due to addition of low amount of CNF (up to 0.7% w/w) in epoxy resin no large clumps of nanofiller was observed by SEM in present study. Thus at all concentrations of CNF mechanical properties were enhanced as compared to neat epoxy film.

4. Conclusions

CNF were successfully isolated from *G. scortechinii* by combination of pulping, bleaching, and hydrolysis. SEM and FT-IR analysis revealed that each step of chemomechanical process contributed to removal of wax, hemicellulose, and

lignin from the treated fiber and this resulted in decrease in fiber diameter as confirmed by TEM. Diameter of extracted CNF was ranging from 5 to 10 nm. Crystallinity of fiber increased during chemomechanical process due to removal of amorphous regions from cellulose. Thermogravimetric analysis explained that the isolated nanofibers exhibited maximal thermal stability, where the highest T_{max} value was 376°C. Mechanical properties like tensile strength and modulus as well as flexural strength and modulus of the nanocomposites improved with addition of CNF loading from 0 to 0.7%. However, elongation at break decreased with increased in CNF concentration in epoxy resin. The SEM fracture surface of CNF reinforced nanocomposites showed rough surface compared to the neat epoxy composite. At 0.7% of CNF agglomeration was observed. Overall, it can be concluded that isolated CNF from *G. scortechinii* bamboo can be a suitable alternative reinforcing agent or filler in functional composite, especially epoxy resin for various engineering applications.

Competing Interests

The authors declare that there is no conflict of interests regarding the publication of this paper.

Acknowledgments

The authors would like to thank the Universiti Sains Malaysia for the awarded Postdoctoral Fellowship. The authors gratefully acknowledge Universiti Sains Malaysia, Penang, Malaysia, for providing Research University Grant (RUI-1001/PTEKIND/814255).

References

[1] H. P. S. Abdul Khalil, P. Amouzgar, M. Jawaid et al., "New approach to oil palm trunk core lumber material properties enhancement via resin impregnation," *Journal of Biobased Materials and Bioenergy*, vol. 6, no. 3, pp. 299–308, 2012.

[2] K. Wong, "Current and potential uses of bamboo in Peninsular Malaysia," *Journal of the American Bamboo Society*, vol. 7, no. 172, pp. 1–15, 1989.

[3] M. T. Mustafa, R. Wahab, M. Sudin, I. Khalid, and N. A. M. Kamal, "Anatomical properties and microstructures features of four cultivated bamboo *Gigantochloa* species," *Asian Journal of Scientific Research*, vol. 1, no. 7, pp. 328–339, 2011.

[4] H. Ku, H. Wang, N. Pattarachaiyakoop, and M. Trada, "A review on the tensile properties of natural fiber reinforced polymer composites," *Composites Part B: Engineering*, vol. 42, no. 4, pp. 856–873, 2011.

[5] H. P. S. A. Khalil, N. A. S. Aprilia, A. H. Bhat, M. Jawaid, M. T. Paridah, and D. Rudi, "A Jatropha biomass as renewable materials for biocomposites and its applications," *Renewable and Sustainable Energy Reviews*, vol. 22, pp. 667–685, 2013.

[6] H. P. S. A. Khalil, N. Z. Noriman, M. N. Ahmad, M. M. Ratnam, and N. A. N. Fuaad, "Polyester composites filled carbon black and activated carbon from bamboo (*Gigantochloa scortechinii*): physical and mechanical properties," *Journal of Reinforced Plastics and Composites*, vol. 26, no. 3, pp. 305–320, 2007.

[7] M. S. Alwani, H. P. S. A. Khalil, O. Sulaiman, M. N. Islam, and R. Dungani, "An approach to using agricultural waste fibres in biocomposites application: thermogravimetric analysis and activation energy study," *BioResources*, vol. 9, no. 1, pp. 218–230, 2014.

[8] Y. F. Shih, "Mechanical and thermal properties of waste water bamboo husk fiber reinforced epoxy composites," *Materials Science and Engineering: A*, vol. 445-446, pp. 289–295, 2007.

[9] H. P. S. Abdul Khalil, B. T. Poh, M. Jawaid et al., "The effect of soil burial degradation of oil palm trunk fiber-filled recycled polypropylene composites," *Journal of Reinforced Plastics & Composites*, vol. 29, no. 11, pp. 1653–1663, 2010.

[10] H. A. S. Abdul Khalil, N. L. Suraya, N. Atiqah, M. Jawaid, and A. Hassan, "Mechanical and thermal properties of chemical treated kenaf fibres reinforced polyester composites," *Journal of Composite Materials*, vol. 47, no. 26, pp. 3343–3350, 2013.

[11] K. O. Reddy, C. U. Maheswari, M. Shukla, J. I. Song, and A. Varada Rajulu, "Tensile and structural characterization of alkali treated Borassus fruit fine fibers," *Composites Part B: Engineering*, vol. 44, no. 1, pp. 433–438, 2013.

[12] M. Jawaid, O. Y. Alothman, M. T. Paridah, and H. P. S. Abdul Khalil, "Effect of oil palm and jute fiber treatment on mechanical performance of epoxy hybrid composites," *International Journal of Polymer Analysis and Characterization*, vol. 19, no. 1, pp. 62–69, 2014.

[13] D. Klemm, D. Schumann, F. Kramer, N. Hebler, D. Koth, and B. Sultanova, "Nanocellulose materials—different cellulose, different functionality," *Macromolecular Symposia*, vol. 280, no. 1, pp. 60–71, 2009.

[14] W. Stelte and A. R. Sanadi, "Preparation and characterization of cellulose nanofibers from two commercial hardwood and softwood pulps," *Industrial and Engineering Chemistry Research*, vol. 48, no. 24, pp. 11211–11219, 2009.

[15] B. Wang and M. Sain, "Dispersion of soybean stock-based nanofiber in a plastic matrix," *Polymer International*, vol. 56, no. 4, pp. 538–546, 2007.

[16] H. P. S. Abdul Khalil, M. S. Hossain, E. Rosamah et al., "High-pressure enzymatic hydrolysis to reveal physicochemical and thermal properties of bamboo fiber using a supercritical water fermenter," *BioResources*, vol. 9, no. 4, pp. 7710–7720, 2014.

[17] N. A. Sri Aprilia, M. S. Hossain, M. Asniza et al., "Optimizing the isolation of microfibrillated bamboo in high pressure enzymatic hydrolysis," *BioResources*, vol. 10, no. 3, pp. 5305–5316, 2015.

[18] I. Y. A. Fatah, H. P. S. Abdul Khalil, M. S. Hossain et al., "Exploration of a chemo-mechanical technique for the isolation of nanofibrillated cellulosic fiber from oil palm empty fruit bunch as a reinforcing agent in composites materials," *Polymers*, vol. 6, no. 10, pp. 2611–2624, 2014.

[19] W. He, S. Jiang, Q. Zhang, and M. Pan, "Isolation and characterization of cellulose nanofibers from *Bambusa rigida*," *BioResources*, vol. 8, no. 4, pp. 5678–5689, 2013.

[20] M. Jonoobi, K. O. Niska, J. Harun, and M. Misra, "Chemical composition, crystallinity, and thermal degradation of bleached and unbleached kenaf bast (*Hibiscus cannabinus*) pulp and nanofibers," *BioResources*, vol. 4, no. 2, pp. 626–639, 2009.

[21] C. H. Chan, C. H. Chia, S. Zakaria, I. Ahmad, and A. Dufresne, "Production and characterisation of cellulose and nano- crystalline cellulose from kenaf core wood," *BioResources*, vol. 8, no. 1, pp. 785–794, 2013.

[22] M. Jonoobi, A. Khazaeian, P. M. Tahir, S. S. Azry, and K. Oksman, "Characteristics of cellulose nanofibers isolated from

rubberwood and empty fruit bunches of oil palm using chemo-mechanical process," *Cellulose*, vol. 18, no. 4, pp. 1085–1095, 2011.

[23] Y. Nishiyama, J. Sugiyama, H. Chanzy, and P. Langan, "Crystal structure and hydrogen bonding system in cellulose Iα from synchrotron X-ray and neutron fiber diffraction," *Journal of the American Chemical Society*, vol. 125, no. 47, pp. 14300–14306, 2003.

[24] A. Alemdar and M. Sain, "Isolation and characterization of nanofibers from agricultural residues—wheat straw and soy hulls," *Bioresource Technology*, vol. 99, no. 6, pp. 1664–1671, 2008.

[25] A. Omrani, L. C. Simon, and A. A. Rostami, "Influences of cellulose nanofiber on the epoxy network formation," *Materials Science and Engineering A*, vol. 490, no. 1-2, pp. 131–137, 2008.

[26] H. P. S. Abdul Khalil, H. M. Fizree, A. H. Bhat, M. Jawaid, and C. K. Abdullah, "Development and characterization of epoxy nanocomposites based on nano-structured oil palm ash," *Composites Part B: Engineering*, vol. 53, pp. 324–333, 2013.

[27] K.-Y. Lee, Y. Aitomäki, L. A. Berglund, K. Oksman, and A. Bismarck, "On the use of nanocellulose as reinforcement in polymer matrix composites," *Composites Science and Technology*, vol. 105, pp. 15–27, 2014.

[28] M. Jonoobi, J. Harun, A. P. Mathew, and K. Oksman, "Mechanical properties of cellulose nanofiber (CNF) reinforced polylactic acid (PLA) prepared by twin screw extrusion," *Composites Science and Technology*, vol. 70, no. 12, pp. 1742–1747, 2010.

[29] R. Masoodi, R. F. El-Hajjar, K. M. Pillai, and R. Sabo, "Mechanical characterization of cellulose nanofiber and bio-based epoxy composite," *Materials and Design*, vol. 36, pp. 570–576, 2012.